JIAS

Journal of Intelligent Automation Systems
Published online: 15 January 2014

Combined NN/RISE-based Asymptotic Tracking Control of a 3 DOF Robot Manipulator

Sara Yazdanzad[a], Alireza Khosravi[b,*], Abolfazl Ranjbar Noei[c] and Alireza Alfi[d]

Abstract: Robotic control is an interesting subject due to its extensive industrial applications. This paper proposes a new continuous control design for tracking problem of a three degree-of-freedom (DOF) robot manipulator in presence of uncertainties and bounded external disturbances. The proposed method is based on the combination of the recently developed robust integral of the sign of the error (RISE) feedback and neural network (NN) feed forward terms. In this control strategy, a feed forward NN is utilized to compensate uncertainties of the nonlinear system. Furthermore, the RISE feedback control term is used to eliminate the NN approximation error and bounded external disturbances. Typical NN-based controllers generally provide the convergence only with uniformly ultimately bounded (UUB) error due to the NN reconstruction error. However, the proposed method guarantees asymptotic tracking by eliminating this error. Using Lyapunov stability analysis, a semi-global asymptotic tracking of the robot joints is achieved. Besides, a comparative study on the system performance is conducted between the proposed control strategy and an NN-based controller. Simulation results demonstrate that the proposed controller is robust to deal with uncertainties, and verify the effectiveness of the proposed control scheme.

Keywords: Feed forward neural network, RISE feedback, Asymptotic tracking, three-link robot.

1. Introduction

In the past few decades, design of tracking controller for robot manipulators has received significant attention. Several model based methods have been proposed for the tracking problem of robotic systems. These methods require an accurate dynamic model of system. Robot manipulators are complex nonlinear dynamic systems. In fact, it is difficult to attain an exact mathematical model of the robot, due to the existence of uncertain elements such as nonlinear friction, payload variation, flexibility of the joints and unknown disturbances. Hence, it is necessary to design a controller which is robust against the mentioned uncertainties and presents an appropriate tracking performance. Several research efforts have been conducted over the past two decades, and different control strategies have been introduced

a Department of Electrical and Computer Engineering, Noshirvani University of Technology, Babol, Iran
**Corresponding author. b Department of Electrical and Computer Engineering, Noshirvani University of Technology, Babol, Iran, phone: +98-111-3239214; fax: +98-111-3239214; e-mail: akhosravi@nit.ac.ir*
c Department of Electrical and Computer Engineering, Noshirvani University of Technology, Babol, Iran
d Deparment of Electrical and Robotic Engineering, Shahrood, University of Technology, shahrood, Iran

for tracking control of robot manipulators such as computed torque control [1], adaptive control techniques [2, 3], sliding mode control (SMC) [4, 5, 6], and robust control strategy [7, 8].

Computed torque control scheme requires an accurate dynamic model of plant. Moreover, the existence of uncertainties in the dynamic model degrades the performance of this technique. Robust control is a common control strategy to achieve good tracking performance for robot manipulators in the presence of uncertainties. To design a controller using this method, the bounds of uncertainties should be known in advance, and usually are hard to achieve. Hence, conservative estimated bounds are mostly in use. However, the implementation of the control law, based on these conservative bounds, leads to degradation of control performance due to receiving unnecessarily high feedback selection. Adaptive controllers are suitable to apply on nonlinear systems with parametric uncertainties and bounded disturbances. Indeed, this technique presents precise tracking performance in the presence of uncertainties. However, it is often confined to systems that are linear in the unknown parameters. Moreover, it requires an accurate dynamic model of system to determine the regression matrix. Furthermore, a new regression matrix must be computed for any specified plant which involves tedious computations.

Sliding mode control is an efficient robust control strategy to control uncertain nonlinear systems [9]. But this method has some disadvantages such as: appearance of the destructive chattering phenomenon due to the discontinuous nature of the control law [10], requiring a comprehensive knowledge of the system dynamics [11] that is difficult to obtain in most cases, and the necessity of knowing bounds of uncertainties to attain robust characteristics. To overcome these drawbacks, several approaches have been developed. The most common approach for chattering reduction is to define a boundary layer around the sliding surface and then use a continuous approximation of the switching control input within the boundary layer [12]. This approach can reduce the chattering effectively, but there is a trade-off between asymptotic tracking and the elimination of chattering for the width of the boundary layer. Fuzzy boundary layers can be employed to reduce the chattering [13]. Although these techniques improve system performance, they tend to increase the complexity of system dynamics.

In recent years, utilization of neural networks in control of robot manipulators has been greatly studied by many researchers. Actually, neural networks are able to approximate nonlinear continuous functions. Hence, they are powerful tools to compensate for uncertainties and control of robotic systems [14, 15, 16]. Lewis et al. [17] proposed a multilayer neural network controller for a general serial-link rigid robot which guarantees tracking performance. Although this type of controllers can achieve good performance without requirement of prior accurate knowledge of dynamic system, existence of the NN functional reconstruction error leads to uniformly ultimately bounded (UUB) stability results [18, 19]. To eliminate the NN reconstruction error, Tang et al. designed an NN controller using sliding mode. However the work led to an undesirable chattering phenomenon as a result of using discontinuous controller [20]. In this study, a recently developed robust integral of the sign of the error (RISE) feedback term is integrated into the NN feed forward compensator to overcome the NN reconstruction error.

Recently, a new feedback control scheme called robust integral of the sign of the error is proposed [21]. This control strategy has been extensively studied because it can compensate for additive disturbances and uncertainties under the assumption that the disturbances are C^2 with bounded time derivatives by generating a continuous control signal [22, 23]. Patre et al. utilized this method to develop a tracking controller for a class of uncertain nonlinear systems [24]. The RISE method is a high gain feedback tool. Motivated by this issue a feed forward element is combined with the RISE feedback structure in order to reduce the gain values of the RISE feedback [25, 26]. Also, Shicheng Wang et al. designed a RISE based NN controller for a spacecraft formation within the leader follower architecture [27].

In this paper, a novel control design is presented for the tracking problem of a three-link robot manipulator in the presence of uncertainties and bounded external disturbances. The method is a combination of an NN feed forward element and the RISE feedback control term. The feed forward NN approximates nonlinear dynamics of the system and compensates for uncertainties. However, due to the NN approximation error, an asymptotic tracking of the desired trajectory usually fails. Therefore, the RISE feedback control term is employed as a part of the control scheme to eliminate the NN approximation error and achieve semi-global asymptotic tracking.

The rest of this paper is organized as follows: Section 2 presents the characteristics of a dynamical model of a three-link robot manipulator. Then, in Section 3, multilayer feed forward neural network and the way for using it, is described. In Section 4, the proposed combined NN-RISE controller is introduced and semi-global asymptotic tracking is analytically achieved using the Lyapunov stability analysis. In Section 5, simulation results on a three-link robot manipulator show a satisfactory performance of the proposed scheme. Finally, Section 6 presents some concluding remarks.

2. Mathematical model for a three-link robot manipulator

The dynamics of a general rigid link manipulator having n degree of freedom in free space, is as follows:

$$\boldsymbol{M(q)\ddot{q} + C(q,\dot{q})\dot{q} + G(q) + \tau_d(t) = \tau(t)} \quad (1)$$

This dynamic equation is obtained by using the Euler-Lagrangian approach. In (1) for the three-link rigid robot manipulator, $q(t), \dot{q}(t), \ddot{q}(t) \in R^3$ are the position, velocity and acceleration of the joints, respectively. $M(q) \in R^{3\times3}$ is the positive definite inertia matrix, $C(q,\dot{q}) \in R^{3\times3}$ represents the Coriolis/centripetal matrix, and $G(q) \in R^3$ expresses the gravity vector. $\tau_d(t) \in R^3$ denotes the vector of disturbances and unmodeled dynamics, and $\tau(t) \in R^3$ denotes the input torque vector applied to the joints. Figure 1 shows the three link robot manipulator. In the following, it is assumed that $q(t)$ and $\dot{q}(t)$ are measurable and $M(q), C(q,\dot{q}), G(q)$ and $\tau_d(t)$ are unknown. The dynamic model (1) of the robot has the following properties:

Property 1: The inertia matrix $M(q)$ is symmetric, positive definite, and holds the following inequality true:

$$m_1\|y\|^2 \le y^T M(q) y \le \bar{m}(q)\|y\|^2 \ \ \forall y \in R^3 \quad (2)$$

where $m_1 \in R$ is a known positive constant, $\bar{m}(q) \in R$ is a known positive function and $\|.\|$ represents the standard Euclidean norm.

Property 2: The nonlinear disturbance term and its first two time derivatives are bounded i.e. $\tau_d(t), \dot{\tau}_d(t), \ddot{\tau}_d(t) \in \mathcal{L}_\infty$.

Property 3: If $q(t), \dot{q}(t) \in \mathcal{L}_\infty$, then $C(q,\dot{q}), G(q)$ are bounded. Further, if $q(t), \dot{q}(t) \in \mathcal{L}_\infty$, then the first and second partial derivatives of the elements of $M(q), C(q,\dot{q}), G(q)$ with respect to $q(t)$ exist and are bounded. In addition, the first and second partial derivatives of the elements of $C(q,\dot{q})$ with respect to $\dot{q}(t)$ exist and are bounded as well.

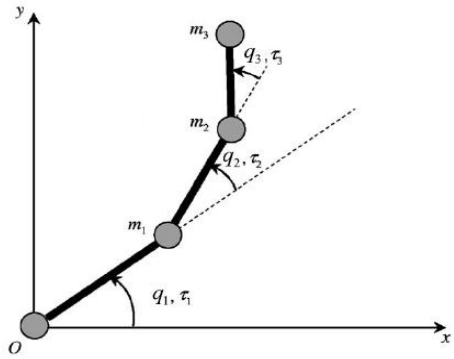

Fig. 1. Three-link planar robot

3. Feed forward neural network

It has been shown that a feed forward NN with at least two layers can approximate any given smooth function on a compact set with any degree of accuracy [15]. This property is called the universal function approximation. It is an important property that empowers the NNs in closed-loop control applications, especially when the dynamic model of system includes nonlinear disturbances and uncertain elements. Let $f(x): R^{N_1+1} \to R^n$ denotes a smooth function. Then for a given compact set $S \in R^{N_1+1}$ and a positive number ε_N, there is an NN having at least two layers, with sufficiently large number of neurons L in hidden layer such that:

$$f(x) = W^T \sigma(V^T x) + \varepsilon(x) \quad (3)$$

where $\varepsilon(x)$ is the NN function approximation error such that $\|\varepsilon\| < \varepsilon_N$ for all given inputs $x \in S$ [15, 30]. In (3), $V \in R^{(N_1+1)\times N_2}$ and $W \in R^{(N_2+1)\times n}$ are bounded constant ideal weight matrices for the input to hidden layer and the hidden to output layer, respectively, where N_1 is the number of input-layer neurons, N_2 is the number of hidden-layer neurons and n is the number of output-layer neurons. $\sigma(.): R^{N_2+1} \to R^{N_2+1}$ is an activation function in the hidden layer. The input vector $x(t)$ and the activation function $\sigma(.)$ are augmented by "1", such that the first column of the weight matrices V and W are considered as thresholds for the first and second layers [15, 30]. Therefore, any tuning of V and W contains tuning of thresholds.

Now based on (3), the NN functional estimate of $f(x)$ is as follows:

$$\hat{f}(x) \triangleq \widehat{W}^T \sigma(\hat{V}^T x) \quad (4)$$

where $\hat{V}(t) \in R^{(N_1+1)\times N_2}$ and $\widehat{W}(t) \in R^{(N_2+1)\times n}$ are the estimates of the ideal weight matrices.

The weight estimation errors, denoted by $\tilde{V}(t) \in R^{(N_1+1)\times N_2}$ and $\tilde{W}(t) \in R^{(N_2+1)\times n}$, are defined as follows:

$$\tilde{V} \triangleq V - \hat{V}\ , \tilde{W} \triangleq W - \widehat{W} \tag{5}$$

and the hidden-layer output error for a given input $x(t)$, denoted by $\tilde{\sigma}(x) \in R^{N_2+1}$, is defined as follows:

$$\tilde{\sigma} \triangleq \sigma - \hat{\sigma} = \sigma(V^T x) - \sigma(\hat{V}^T x) \tag{6}$$

Property 4: (Boundedness of the ideal weights) Based on the assumption that the ideal weights exist and are bounded by known positive values, the following inequalities hold:

$$\|V\|_F{}^2 = tr(V^T V) \le \bar{V}_B \tag{7}$$

$$\|W\|_F{}^2 = tr(W^T W) \le \bar{W}_B \tag{8}$$

where $\|.\|_F$ and $tr(.)$ are the Frobenius norm and the trace of a matrix, respectively.

4. Controller design

In this section, combination of NN feed forward compensator and RISE feedback controller with the objective of guaranteeing semi-global asymptotic tracking is described.

4.1. Control objective

The objective is to design a controller for the robot manipulator that guarantees tracking of a desired trajectory which is denoted by $q_d(t) \in R^n$, in spite of uncertainties and bounded disturbances. To formulate this objective, a position tracking error, denoted by $e_1(t) \in R^n$, is defined as:

$$e_1 \triangleq q_d - q \tag{9}$$

It is assumed that the desired trajectory is designated such that $q_d{}^{(i)}(t) \in \mathscr{L}_\infty, i = 1,2,\dots,5$. Moreover, the filtered tracking errors are denoted by $e_2(t), r(t) \in R^n$, which is defined as follows:

$$e_2 \triangleq \dot{e}_1 + \alpha_1 e_1 \tag{10}$$

$$r \triangleq \dot{e}_2 + \alpha_2 e_2 \tag{11}$$

where $\alpha_1 \in R^{n\times n}$ is a positive constant matrix and $\alpha_2 \in R$ is a positive constant.

4.2. Open-loop error system

Multiplying both sides of (11) by $M(q)$ and then using (1), (9) and (10) into it, the open-loop error system is yielded as follows:

$$\begin{aligned} M(q)r = N(q_d, \dot{q}_d, \ddot{q}_d) + S(q, \dot{q}, q_d, \dot{q}_d, \ddot{q}_d) \\ + \tau_d - \tau \end{aligned} \tag{12}$$

where the auxiliary functions $N(q_d, \dot{q}_d, \ddot{q}_d)$ and $S(q, \dot{q}, q_d, \dot{q}_d, \ddot{q}_d)$ are defined as:

$$N \triangleq M(q_d)\ddot{q}_d + C(q_d, \dot{q}_d)\dot{q}_d + G(q_d) \tag{13}$$

$$\begin{aligned} S \triangleq M(q)(\alpha_1 \dot{e}_1 + \alpha_2 e_2) + C(q, \dot{q})\dot{q} \\ + G(q) + M(q)\ddot{q}_d - N \end{aligned} \tag{14}$$

The expression in (13) can be represented by a three-layer NN as in the following:

$$N = W^T \sigma(V^T x_d) + \varepsilon(x_d) \tag{15}$$

where the input $x_d(t) \in R^{3n+1}$ is defined as $x_d \triangleq [1\ q_d^T(t)\ \dot{q}_d^T(t)\ \ddot{q}_d^T(t)]^T$, so that $N_1 = 3n$ where N_1 was introduced in (3).

Based on the assumption that the desired trajectory is bounded, the following inequalities are hold:

$$\begin{aligned} \|\varepsilon(x_d)\| \le \varepsilon_{b_1}, \|\dot{\varepsilon}(x_d, \dot{x}_d)\| \\ \le \varepsilon_{b_2}, \|\ddot{\varepsilon}(x_d, \dot{x}_d, \ddot{x}_d)\| \\ \le \varepsilon_{b_3} \end{aligned} \tag{16}$$

where $\varepsilon_{b_1}, \varepsilon_{b_2}, \varepsilon_{b_3} \in R$ are known positive constants.

4.3. Closed-loop error system

In the previous section, a neural network is utilized to estimate uncertain nonlinear dynamics of the robot. It should be noted that, the existence of NN functional approximation error leads to UUB stability [15, 31]. The equilibrium point x_e is said to be uniformly ultimately bounded if there exists a compact set $S \subset R^n$ so that for all $x_0 \in S$ there exist a bound B and a time $T(B, x_0)$ such that $\|x(t) - x_e\| \le B$ for all $t \ge t_0 + T$. Figure 2 shows this definition. In fact, ultimate boundedness reveals the fact that the trajectory $x(t)$ starting from x_0 at time t_0 will ultimately enter and remain in the set S. In other words, the difference between the trajectory$x(t)$ and the equilibrium point x_e remains bounded.

The UUB stability results due to NN functional approximation error for NN controllers, has previously been studied in literature. For more details see [15]. In this paper, in order to eliminate this error, the NN-based feed forward method is augmented by the RISE feedback control term, $\mu(t) \in R^n$, which is defined as follows [21]:

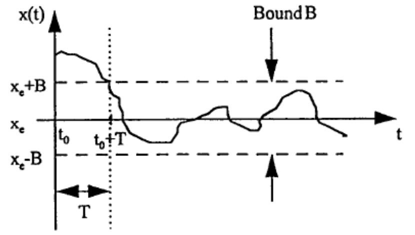

Fig. 2. Illustration of uniform ultimate boundedness

$$\mu(t) \triangleq (k_s+1)e_2(t) - (k_s+1)e_2(0) + \int_0^t [(k_s+1)\alpha_2 e_2(\sigma) + \beta_1 sgn(e_2(\sigma))]d\sigma \quad (17)$$

where its time derivative is expressed by:

$$\dot{\mu}(t) = (k_s+1)r + \beta_1 sgn(e_2) \quad (18)$$

In (17), $k_s, \beta_1 \in R$ are positive constant control gains. A schematic diagram of the proposed control structure is shown in Figure 3.

Therefore, based on the open-loop error system in (12), the control torque input is composed of two components, an NN feed forward term and the RISE feedback control term as below:

$$\tau = \hat{N} + \mu \quad (19)$$

where the NN component, $\hat{N}(t) \in R^n$, is as follows:

$$\hat{N} \triangleq \hat{W}^T \sigma(\hat{V}^T x_d) \quad (20)$$

The adaptation law for the estimates of the ideal weight matrices, $\hat{W}$ and $\hat{V}$, are as follows:

$$\dot{\hat{W}} \triangleq proj(\Gamma_1 \hat{\sigma}' \hat{V}^T \dot{x}_d {e_2}^T) \quad (21)$$

$$\dot{\hat{V}} \triangleq proj(\Gamma_2 \dot{x}_d ({\hat{\sigma}'}^T \hat{W} e_2)^T) \quad (22)$$

where $\Gamma_1 \in R^{(N_2+1)\times(N_2+1)}$ and $\Gamma_2 \in R^{(N_1+1)\times(N_1+1)}$ are constant, positive definite, symmetric control gain matrices. The operator $proj(.)$ denotes the projection algorithm [28]. The projection algorithm for two vectors $\theta, y \in R^n$ is as follows:

$$\dot{\theta} = proj(\theta, y) = \begin{cases} y - \dfrac{\nabla f(\theta)(\nabla f(\theta))^T}{\|\nabla f(\theta)\|^2} y f(\theta) & if\ f(\theta) > 0\ and\ y^T \nabla f(\theta) > 0 \\ y & otherwise \end{cases} \quad (23)$$

where $f: R^n \to R$ is a convex function and $\nabla f(\theta) = (\frac{\partial f(\theta)}{\partial \theta_1} \dots \frac{\partial f(\theta)}{\partial \theta_n})^T$. In fact, this algorithm ensures that the parameter θ remains bounded. Accordingly, this algorithm is used to guarantee the boundedness of the estimated weights of the NN ($\hat{W}$ and $\hat{V}$).

By substituting the control input (19) into (12), the closed-loop tracking error system is achieved as follows:

$$M(q)r = N - \hat{N} + S + \tau_d - \mu \quad (24)$$

By differentiating the equation (24), and
:

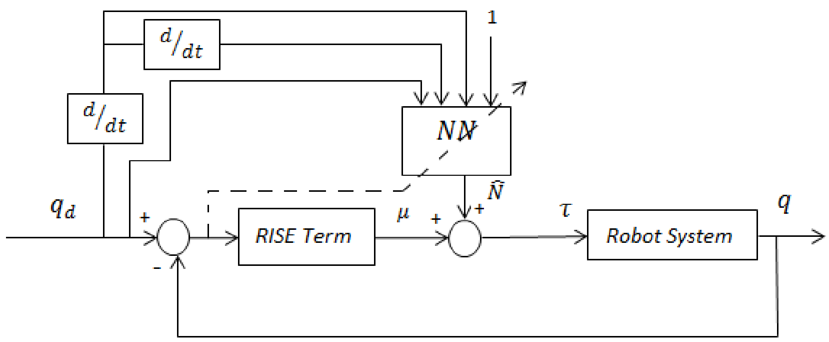

Fig. 3. Block diagram of the control scheme

substituting (15) and (20) into it, then adding and subtracting the terms $W^T \hat{\sigma}' \hat{V}^T \dot{x}_d + \hat{W}^T \hat{\sigma}' \tilde{V}^T \dot{x}_d$ to the resulted equation, and substituting (18), (21) and (22) into it, the following equation can be obtained.

$$M(q)\dot{r} = -\frac{1}{2}\dot{M}(q)r + \tilde{Q} + Q - e_2 - (k_s+1)r - \beta_1 sgn(e_2) \quad (25)$$

where

$$\tilde{Q} \triangleq \quad (26)$$

$$-\frac{1}{2}\dot{M}(q)r - proj\left(\Gamma_1\hat{\sigma}'\hat{V}^T\dot{x}_d e_2{}^T\right)^T\hat{\sigma} - \widehat{W}^T\hat{\sigma}' proj\left(\Gamma_2\dot{x}_d\left(\hat{\sigma}'^T\widehat{W}e_2\right)^T\right)^T x_d + \dot{S} + e_2$$

and in a similar manner as in [24], Q is separated as:

$$Q \triangleq Q_d + Q_B \tag{27}$$

$$Q_d \triangleq W^T\sigma' V^T\dot{x}_d + \dot{\varepsilon} + \dot{\tau}_d \tag{28}$$

$$Q_B \triangleq Q_{B_1} + Q_{B_2} \tag{29}$$

$$Q_{B_1} \triangleq -W^T\hat{\sigma}'\hat{V}^T\dot{x}_d - \widehat{W}^T\hat{\sigma}'\tilde{V}^T\dot{x}_d \tag{30}$$

$$Q_{B_2} \triangleq \widehat{W}^T\hat{\sigma}'\tilde{V}^T\dot{x}_d + \widetilde{W}^T\hat{\sigma}'\hat{V}^T\dot{x}_d \tag{31}$$

Using the Mean Value Theorem, Property 2, (7), (8), (16), (21), (22), (29)-(31), the following inequalities are hold:

$$\|\tilde{Q}\| \le \rho(\|z\|)\|z\|$$
$$\|Q_d\| \le \xi_1, \|Q_B\| \le \xi_2, \|\dot{Q}_d\| \le \xi_3$$
$$\|\dot{Q}_B\| \le \xi_4 + \xi_5\|e_2\| \tag{32}$$

where $z(t) \in R^{3n}$ is defined as:

$$z(t) \triangleq [e_1^T \;\; e_2^T \;\; r^T]^T \tag{33}$$

and the function $\rho(\|z\|) \in R$ is a positive globally invertible nondecreasing function. Also $\xi_i \in R, i = 1,2,3,4,5$ are known positive constants.

4.4. Stability analysis

Theorem: The proposed controller in (19) guarantees that all system signals are bounded under closed-loop operation, and the position tracking error goes to zero as follows:

$$\|e_1(t)\|, \|e_2(t)\|, \|r(t)\| \to 0 \;\; as \;\; t \to \infty \tag{34}$$

The goal can be attained while the RISE feedback control gain k_s introduced in (17), is selected large enough, and β_1 and β_2 are chosen according to the following sufficient conditions

$$\beta_1 > \xi_1 + \xi_2 + \frac{1}{\alpha_2}\xi_3 + \frac{1}{\alpha_2}\xi_4 \,, \beta_2 > \xi_5 \tag{35}$$

where $\xi_i \in R, i = 1,2,3,4,5$ are introduced in (32) and β_2 will be introduced in the proof.
Proof: See the Appendix A.

5. Simulation results

In this section, a simulation of the tracking control of a three-link planar robot manipulator is performed to evaluate the validity of the proposed structure. Furthermore, a comparative study on the system performance is conducted between the proposed control strategy and an NN-based controller to illustrate superiority of the proposed scheme.

For the three-link robot manipulator shown in Figure 1, the inertia matrix $M(q)$, the Coriolis/centripetal matrix $C(q,\dot{q})$ and the gravity vector $G(q)$ are as follows[29]:

$$M(q,\dot{q}) = \begin{bmatrix} M_{11} & M_{12} & M_{13} \\ M_{21} & M_{22} & M_{23} \\ M_{31} & M_{32} & M_{33} \end{bmatrix}$$

with

$$M_{11} = 2(d_1 + d_2 + d_3) + 2d_4c_2 + 2d_5c_{23} + 2d_6c_3$$

$$M_{12} = 2(d_2 + d_3) + d_4c_2 + d_5c_{23} + 2d_6c_3$$

$$M_{13} = 2d_3 + d_5c_{23} + d_6c_3$$

$$M_{21} = M_{12}$$

$$M_{22} = 2(d_2 + d_3) + 2d_6c_3$$

$$M_{23} = 2d_3 + d_6c_3$$

$$M_{31} = M_{13} \;\; , \;\; M_{32} = M_{23} \;\; , \;\; M_{33} = 2d_3$$

and

$$C(q,\dot{q})\dot{q} = \begin{bmatrix} C_{11} & C_{12} & C_{13} \\ C_{21} & C_{22} & C_{23} \\ C_{31} & C_{32} & C_{33} \end{bmatrix}\begin{bmatrix} \dot{q}_1 \\ \dot{q}_2 \\ \dot{q}_3 \end{bmatrix}$$

where the $C_{ij}, (i = 1,2,3, \; j = 1,2,3)$ are defined as follows:

$$C_{11} = -\dot{q}_2d_4s_2 - d_5s_{23}(\dot{q}_2 + \dot{q}_3) - d_6s_3\dot{q}_3$$

$$C_{12} = -d_4s_2(\dot{q}_1 + \dot{q}_2) - d_5s_{23}(\dot{q}_1 + \dot{q}_2 + \dot{q}_3) - d_6s_3\dot{q}_3$$

$$C_{13} = -(d_5s_{23} + d_6s_3)(\dot{q}_1 + \dot{q}_2 + \dot{q}_3)$$

$$C_{21} = (d_4s_2 + d_5s_{23})\dot{q}_1 - d_6s_3\dot{q}_3$$

$$C_{22} = -d_6s_3\dot{q}_3$$

$$C_{23} = -d_6s_3(\dot{q}_1 + \dot{q}_2 + \dot{q}_3)$$

$$C_{31} = d_5s_{23}\dot{q}_1 + d_6s_3(\dot{q}_1 + \dot{q}_2)$$

$C_{32} = d_6 s_3(\dot{q}_1 + \dot{q}_2)$

$C_{33} = 0$

and

$$G(q) = \begin{bmatrix} g_1 \\ g_2 \\ g_3 \end{bmatrix}$$

with

$$g_1 = \frac{1}{2}a_1c_1m_1g + \left(a_1c_1 + \frac{1}{2}a_2c_{12}\right)m_2g + (a_1c_1 + a_2c_{12} + \frac{1}{2}a_3c_{123})m_3g$$

$$g_2 = \left(\frac{1}{2}a_2c_{12}\right)m_2g + (a_2c_{12} + \frac{1}{2}a_3c_{123})m_3g$$

$$g_3 = (\frac{1}{2}a_3c_{123})m_3g \quad (36)$$

where $q = [q_1\ q_2\ q_3]^T$ and $\dot{q} = [\dot{q}_1\ \dot{q}_2\ \dot{q}_3]^T$ represent the joints positions and velocities, respectively. Also $s_i, c_i, s_{ij}, c_{ij}, c_{ijk}$ $(i = 1,2,3,\ j = 1,2,3,\ k = 1,2,3)$ denote $\sin(q_i)$, $\cos(q_i)$, $\sin(q_i + q_j)$, $\cos(q_i + q_j)$, $\cos(q_i + q_j + q_k)$, respectively. m_i And $a_i, i = 1,2,3$ are the masses and lengths of the links, respectively, and the parameters $d_i, i = 1, \dots, 6$ are defined as follows [29]:

$$d_1 = \frac{1}{2}[\left(\frac{1}{4}m_1 + m_2 + m_3\right)a_1^2 + I_{o1}]$$

$$d_2 = \frac{1}{2}[\left(\frac{1}{4}m_2 + m_3\right)a_2^2 + I_{o2}]$$

$$d_3 = \frac{1}{2}[\left(\frac{1}{4}m_3\right)a_3^2 + I_{o3}]$$

$$d_4 = (\frac{1}{2}m_2 + m_3)a_1a_2$$

$$d_5 = \frac{1}{2}m_3a_1a_3$$

$$d_6 = \frac{1}{2}m_3a_2a_3 \quad (37)$$

where $I_{oi}, i = 1,2,3$ denotes the moment of inertia of ith joint. The numerical values of the robot dynamical parameters are listed in Table 1 [29].

The control objective is to design a controller to track the desired trajectories $q_d = \left[\sin(t), \cos(t), \sin\left(t + \left({}^{\pi}/_{3}\right)\right)\right]^T$ as desired positions of the first, second and the third joint of the robot, respectively. Furthermore, external disturbances $\tau_{d1} = 0.2\sin(2t)$, $\tau_{d2} = 0.1\cos(2t)$, $\tau_{d3} = 0.1\sin(t)$ are applied to those joints, respectively. The initial position and velocity of the joints are set to zero.

- *First case: NN-based controller design*

The NN-based controller is constructed by [17]:

$$\tau = \widehat{W}^T\sigma\left(\hat{V}^T x\right) + k_v e_2 - v \quad (38)$$

$$\dot{\widehat{W}} = F\hat{\sigma}e_2^T - F\hat{\sigma}'\hat{V}^T x e_2^T - \kappa_w F\|e_2\|\widehat{W} \quad (39)$$

$$\dot{\hat{V}} = Gx(\hat{\sigma}'\widehat{W}^T e_2)^T - \kappa_v G\|e_2\|\hat{V} \quad (40)$$

$$v(t) = -K_z(\|\hat{Z}\|_F + Z_B)e_2 \quad (41)$$

where the NN input, x, is defined as $x = [1, e_1^T, \dot{e}_1^T, q_d^T, \dot{q}_d^T, \ddot{q}_d^T]$, $Z = diag\{W, V\}$ and $\|Z\|_F \leq Z_B$. The feedback control gain matrix

Table 1. Simulation parameters of robot [29]

	Mass m_i **(kg)**	**Link** a_i **(m)**	**Moment of inertia** I_{oi} **(kgm^2)**
Joint 1, i=1	1.2	0.5	43.33×10^{-3}
Joint 2, i=2	1.5	0.4	25.08×10^{-3}
Joint 3, i=3	3	0.3	32.67×10^{-3}

$k_v = 15 \times I^{3\times3}$ and the design parameter matrix $\alpha_1 = 2 \times I^{3\times3}$. The design parameters are also selected as $F = 5 \times I^{10\times10}$, $G = 5 \times I^{16\times16}$, $\kappa_w = 0.1$, $\kappa_v = 0.1$, $K_z = 2$ and $Z_B = 10$. The number of neurons in the hidden layer of the NN is selected as $N_2 = 1$ and its activation function is considered as $logsig(.)$. The initial weights of the first and second layer of NN are set as $5 \times rand(16{,}10)$ and $0.5 \times rand(10{,}3)$.

The results of NN-based controller are shown in Figure 4. Figure 4(a) shows the tracking error for all three joints of the robot. It can be seen that the tracking errors always exist and are uniformly ultimately bounded. In fact, due to the inherent functional reconstruction error of the NN, asymptotically convergence to zero is almost failed. Control efforts of all the joints are shown in Figure 4(b). Moreover, the NN weights norms, for the first and second layers, are shown in Figures 4(c) and 4(d), respectively.

- *Second case: Design of the RISE feedback controller in combination with the NN feedforward term*

In order to design the proposed controller in this paper, the control torque input presented in (19) is utilized. The control gains are chosen as $\alpha_1 = 2 \times I^{3\times3}$, $\alpha_2 = 18$, $k_s = 25$, $\beta_1 = 5$. In this simulation a neural network with $N_2 = 10$ hidden-layer neurons and $n = 3$ output-layer neurons is considered. Initial weights of the first and second layer of the NN are set as $\hat{V} = randn(10{,}10)$ and $\widehat{W} = 10 \times randn(10{,}3)$. The activation function of the NN is also considered as $logsig(.)$. The adaptation gains are selected as $\square_1 = 5 \times I^{10\times10}$, $\square_2 = 0.05 \times I^{10\times10}$. The results of the simulation are shown in Figure 5.

The joints position compared with the desired trajectories are shown in Figure 5(a). It confirms that the control objective is successfully achieved and the system tracks the desired trajectory. Figure 5(b) shows the norm of the NN weight matrices. Figure 5(c) demonstrates the position tracking error which confirms that an asymptotic tracking is achieved for all three joints of the robot. Figure 5(d) shows the

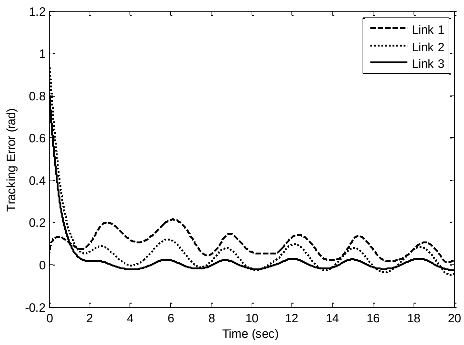

(**a**). Tracking error of joints

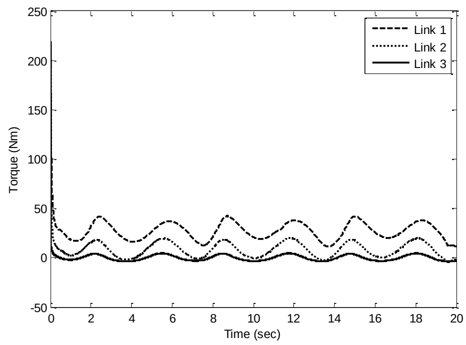

(**b**). Control inputs for joints of the robot

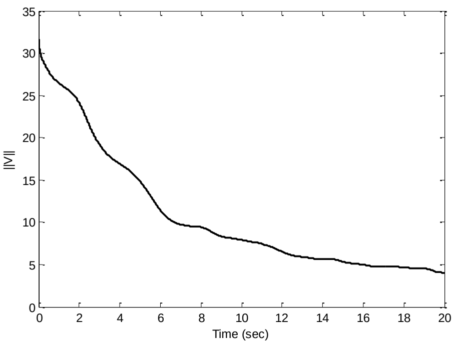

(**c**). Norm of the first layer weights

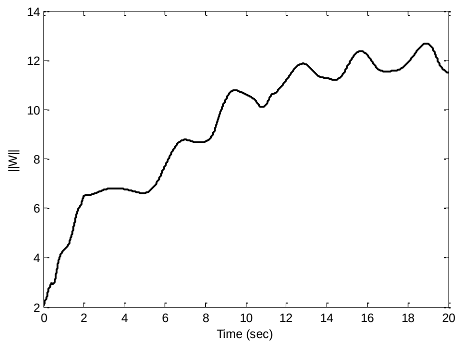

(**d**). Norm of the second layer weights

Fig. **4**.The results of NN-based controller in terms of the error (a), torque inputs (b) and norm of the first and second layer weight estimates (c and d)

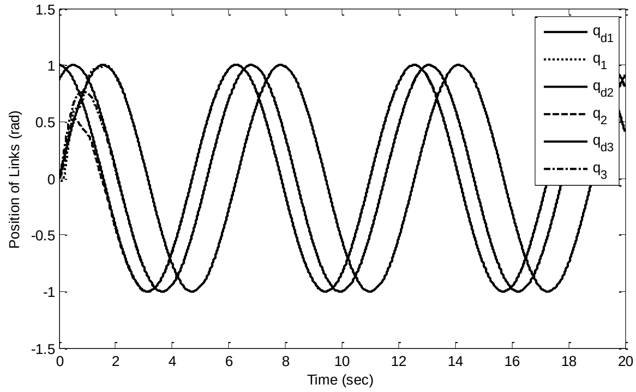

(a). Trajectory tracking of joints

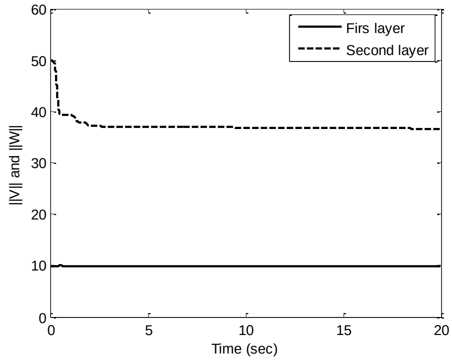

(b). Norm of the first and second layer weight matrices

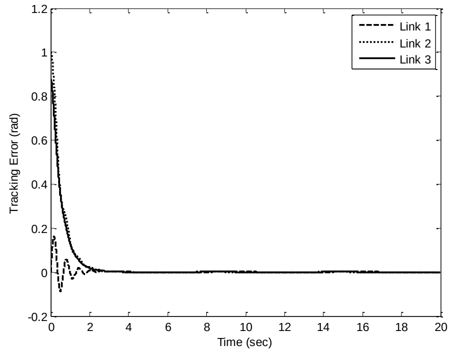

(c). Tracking error of joints

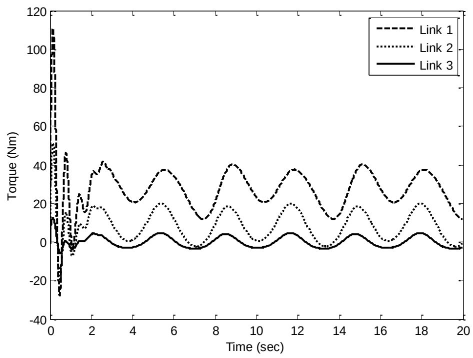

(d). Control inputs for joints of the robot

Fig. 1. The results of the designed controller in this paper in terms of the tracking performance (a), the norm of the first and second layer weight estimates (b), the error (c) and torque inputs (d)

generated control torque input. As it can be seen, the proposed controller generates a continuous control signal which avoids the occurrence of undesirable chattering phenomenon. By comparing Figure 4(a) with Figure 5(c), it can be seen that unlike the NN-based controller which yields UUB results, the proposed control scheme presents asymptotic tracking of course in better performance.

6. Conclusion

Robot manipulators are complex systems with highly nonlinear dynamics. The existence of nonlinearities and uncertainties in the dynamic model makes their control more difficult. In this paper, a continuous control scheme is presented for the tracking problem of a three-link manipulator. The proposed method is a combination of the RISE feedback control technique together with a multilayer NN-based feed forward method. The three-layer NN approximates nonlinear dynamics of the robot and compensates for uncertainties without prior knowledge of the system. The RISE feedback term simultaneously eliminates the NN residual reconstruction error and the joints can track desired trajectories with asymptotical performance. The results of the proposed control scheme are compared with an NN-based controller. The Comparative study on the system performance demonstrated that the proposed method yielded superior tracking performance. The NN-based controller provided the convergence only with UUB error due to the NN reconstruction error. However, the proposed method achieves asymptotic tracking by eliminating this error.

Appendix A

Proof:

Let $\mathcal{D} \subset R^{3n+2}$ be a domain containing $\Phi(t) = 0$, where $\Phi(t) \in R^{3n+2}$ is defined as [24]:

$$\Phi(t) \triangleq [z^T(t)\ \sqrt{\mathcal{R}(t)}\ \ \sqrt{\mathcal{Q}(t)}]^T \tag{42}$$

In (42), the auxiliary function $\mathcal{R}(t) \in R$ is defined as:

$$\mathcal{R}(t) \triangleq \beta_1 \sum_{i=1}^{n} |e_{2i}(0)| - e_2(0)^T Q(0) - \int_0^t L(\tau)d\tau \tag{43}$$

where the subscript $i = 1,2,\dots,n$ denotes the i th element of the vector, and the auxiliary function $L(t) \in R$ is defined as:

$$L(t) \triangleq r^T \left(Q_{B_1}(t) + Q_d(t) - \beta_1 \mathrm{sgn}(e_2)\right) + \dot{e}_2(t)^T Q_{B_2}(t) - \beta_2 \|e_2(t)\|^2 \tag{44}$$

where $\beta_2 \in R$ is a positive constant chosen according to the second sufficient condition in (35). The derivative $\dot{\mathcal{R}}(t) \in R$ can be expressed as:

$$\dot{\mathcal{R}}(t) = -L(t) = -r^T \left(Q_{B_1}(t) + Q_d(t) - \beta_1 \mathrm{sgn}(e_2)\right) - \dot{e}_2(t)^T Q_{B_2}(t) + \beta_2 \|e_2(t)\|^2 \tag{45}$$

Provided the sufficient conditions introduced in (35) are satisfied, the following inequality can be obtained:

$$\int_0^t L(\tau)\, d\tau \le \beta_1 |e_{2i}(0)| - e_2(0)^T Q(0) \tag{46}$$

Hence, (46) can be used to conclude that $\mathcal{R}(t) \ge 0$. The auxiliary function $\mathcal{Q}(t) \in R$ in (42) is defined as:

$$\mathcal{Q}(t) \triangleq \frac{\alpha_2}{2} \mathrm{tr}\left(\tilde{W}^T \square_1^{-1} \tilde{W}\right) + \frac{\alpha_2}{2} \mathrm{tr}(\tilde{V}^T \square_2^{-1} \tilde{V}) \tag{47}$$

Since $\square_1$ and $\square_2$ are constant, symmetric, and positive definite matrices and $\alpha_2 > 0$, it is clear that $\mathcal{Q}(t) \ge 0$.

Let $V_L(\Phi, t): \mathcal{D} \times [0, \infty) \to R$ be a continuously differentiable positive definite function defined as:

$$V_L(\Phi, t) \triangleq e_1^T e_1 + \frac{1}{2} e_2^T e_2 + \frac{1}{2} r^T M(q) r + \mathcal{R} + \mathcal{Q} \tag{48}$$

which holds the following inequality true:

$$U_1(\Phi) \le V_L(\Phi, t) \le U_2(\Phi) \tag{49}$$

Provided the sufficient conditions introduced in (35) are satisfied. In (49), the continuous positive definite functions $U_1(\Phi), U_2(\Phi) \in R$ are defined as:

$$U_1(\Phi) \triangleq \lambda_1 \|\Phi\|^2,\ \ U_2(\Phi) \triangleq \lambda_2(q) \|\Phi\|^2 \tag{50}$$

where $\lambda_1, \lambda_2(q) \in R$ are defined as:

$$\lambda_1 \triangleq \frac{1}{2} \min\{1, m_1\}\ , \lambda_2(q) \triangleq \max\{\frac{1}{2} \bar{m}(q), 1\} \tag{51}$$

where $m_1, \bar{m}(q)$ are introduced in (2). After utilizing (10), (11), (18), and (25), the time derivative of (48) can be expressed as:

$$
\begin{aligned}
\dot{V}_L(\Phi, t) = &-2\alpha_1\|e_1\|^2 + 2e_2^T e_1 + r^T\tilde{Q}(t) \\
&- (k_s + 1)\|r\|^2 \\
&- \alpha_2\|e_2\|^2 + \beta_2\|e_2\|^2 \\
&+ \alpha_2 e_2^T\big[\widehat{W}^T\hat{\sigma}'\tilde{V}^T\dot{x}_d \\
&+ \widetilde{W}^T\hat{\sigma}'\hat{V}^T\dot{x}_d\big] \\
&+ \mathrm{tr}\left(\alpha_2\widetilde{W}^T\square_1^{-1}\dot{\widetilde{W}}\right) \\
&+ \mathrm{tr}(\alpha_2\tilde{V}^T\square_2^{-1}\dot{\tilde{V}})
\end{aligned} \tag{52}
$$

Based on the fact that:

$$
e_2^T e_1 \le \frac{1}{2}\|e_1\|^2 + \frac{1}{2}\|e_2\|^2 \tag{53}
$$

and using (21) and (22), the expression in (52) can be simplified as:

$$
\begin{aligned}
\dot{V}_L(\Phi, t) \le r^T\tilde{Q}(t) &- (k_s + 1)\|r\|^2 \\
&- (2\alpha_1 - 1)\|e_1\|^2 \\
&- (\alpha_2 - \beta_2 - 1)\|e_2\|^2
\end{aligned} \tag{54}
$$

Using (32), the expression in (54) can be further bounded as:

$$
\begin{aligned}
\dot{V}_L(\Phi, t) \le -\lambda_3\|z\|^2 &- (k_s\|r\|^2 \\
&- \rho(\|z\|)\|r\|\|z\|)
\end{aligned} \tag{55}
$$

where $\lambda_3 \triangleq \min\{2\alpha_1 - 1, \alpha_2 - \beta_2 - 1, 1\}$, hence, λ_3 is positive if α_1, α_2 are chosen, according to the following sufficient conditions:

$$
\alpha_1 > \frac{1}{2}, \qquad \alpha_2 > \beta_2 + 1 \tag{56}
$$

After completing the squares for the second and third term in (55), the following expression can be obtained:

$$
\begin{aligned}
\dot{V}_L(\Phi, t) &\le -\lambda_3\|z\|^2 + \frac{\rho^2(z)\|z\|^2}{4k_s} \\
&\le -U(\Phi)
\end{aligned} \tag{57}
$$

where $U(\Phi) = \gamma\|z\|^2$, for some positive constant $\gamma \in R$, is a continuous positive semi-definite function that is defined on the following domain:

$$
D \triangleq \{\Phi \in R^{3n+2} \mid \|\Phi\| \le \rho^{-1}(2\sqrt{\lambda_3 k_s})\} \tag{58}
$$

The inequalities in (49) and (57) can be used to show that $V_L(\Phi, t) \in \mathcal{L}_\infty$ in $\mathcal{D}$, hence, $e_1(t), e_2(t), r(t), \mathcal{R}(t), \mathcal{Q}(t) \in \mathcal{L}_\infty$ in $\mathcal{D}$. Given that $e_1(t), e_2(t), r(t) \in \mathcal{L}_\infty$ in $\mathcal{D}$, standard linear analysis methods can be used to prove that $\dot{e}_1(t), \dot{e}_2(t) \in \mathcal{L}_\infty$ in $\mathcal{D}$ from (10) and (11). Since $e_1(t), e_2(t), r(t) \in \mathcal{L}_\infty$ in $\mathcal{D}$, the assumption that $q_d(t), \dot{q}_d(t), \ddot{q}_d(t)$ exists and are bounded can be used along with (9)-(11) to conclude that $q(t), \dot{q}(t), \ddot{q}(t) \in \mathcal{L}_\infty$ in $\mathcal{D}$. Since $q(t), \dot{q}(t) \in \mathcal{L}_\infty$ in $\mathcal{D}$, property 3 can be used to conclude that $M(q), C(q, \dot{q}), G(q) \in \mathcal{L}_\infty$ in $\mathcal{D}$. Therefore, from (1) and property 2, we can show that $\tau(t) \in \mathcal{L}_\infty$ in $\mathcal{D}$. Given that $r(t) \in \mathcal{L}_\infty$ in $\mathcal{D}$, (18) can be used to show that $\dot{\mu} \in \mathcal{L}_\infty$ in $\mathcal{D}$. Since $\dot{q}(t), \ddot{q}(t) \in \mathcal{L}_\infty$ in $\mathcal{D}$, property 3 can be used to show that $\dot{C}(q, \dot{q}), \dot{G}(q), \dot{M}(q) \in \mathcal{L}_\infty$ in $\mathcal{D}$; hence, (25) can be used to show that $\dot{r}(t) \in \mathcal{L}_\infty$. Since $\dot{e}_1(t), \dot{e}_2(t), \dot{r}(t) \in \mathcal{L}_\infty$ in $\mathcal{D}$, the definition for $z(t), U(t)$ can be used to prove that $U(t)$ is uniformly continuous in $\mathcal{D}$. Let $\mathcal{C} \subset \mathcal{D}$ denote a set defined as follows:

$$
\begin{aligned}
\mathcal{C} \triangleq \{\Phi(t) \subset \mathcal{D} \mid &U_2(\Phi(t)) \\
&< \lambda_1(\rho^{-1}(2\sqrt{\lambda_3 k_s}))^2\}
\end{aligned} \tag{59}
$$

[31, Theory. 8.4] can now be invoked to state that:

$$
\gamma\|z(t)\|^2 \to 0 \ \text{ as } \ t \to \infty \ \ \forall\Phi(0) \in \mathcal{C} \tag{60}
$$

Based on the definition of$z(t)$, (60) can be used to show that:

$$
\|e_1(t)\| \to 0 \ \text{ as } \ t \to \infty \ \ \forall\Phi(0) \in \mathcal{C} \tag{61}
$$

References

[1] M. A. Liama, R. Kelly, V. Santiban˜ ez: Stable computed torque control of robot manipulators via fuzzy selftuning, IEEE Trans. Syst. Man Cybern. B, Cybern., **30**(1), 143–150 (2000).

[2] C. C. Cheah, C. Liu & J. J. E. Slotine: Adaptive Tracking Control for Robots with Uncertainties in Kinematic, Dynamic and Actuator Models, IEEE Transactions on Automatic Control, **51**(6), 1024–1029 (2006).

[3] J. K. Åström, B. Wittenmark: A survey of adaptive control applications," in: Proceedings of 34th IEEE Conference on Decision and Control, New Orleans, Louisiana, 649– 654, (1995).

[4] X. Chen, T. Fukuda: Robust sliding-mode tip position control for flexible arms, IEEE Trans. Ind. Electron, **48**(6), 1048–1056, (2001).

[5] Guangjun Liu, A.A. Goldenberg: Uncertainty Decomposition–Based Robust Control of Robot Manipulators, IEEE Trans Control Sys. Technology, **4**, 384–393 (1996).

[6] G. J. Luis Enrique, L. Alexander G., E. J. Bayro-Corrochano: Integral Nested sliding Mode Control for Robotic Manipulators, Proceedings of 17th IFAC World Congress, 9899–9904, (2008).

[7] A. Tesfaye, M. Tomizuka: Robust MIMO Model Following with Application to Trajectory Motion

Control of Robot Arms, Proceedings of 33th IEEE Conference on Decision and Control, Lake Buena Vista. FL, 814–819, December (1994).

[8] Guangjun Liu ,Andrew A. Goldenberg: Robust Control of Robot Manipulators Based on Dynamics Decomposition, IEEE Trans. Robotics and automation, **13**, 783–789, October, (1997).

[9] X. Yu, O. Kaynak: Sliding-Mode Control with Soft Computing: A Survey, IEEE Trans. On Industrial Electronics, **56**(9), 3275–3285 (2009).

[10] J. J. E. Slotine, W. P. Liu: Applied Nonlinear Control, Prentice-Hall, Englewood Cliffs, NJ, 1991.

[11] O. Kaynak, K. Erbatur, M. Ertugrul: The fusion of computationally intelligent methodologies and sliding-mode control: a survey, IEEE Transactions on Industrial Electronics, **48**, 4–17, (2001).

[12] Slotine J. J. E. and Li W: Applied Nonlinear Control, Prentice-Hall, 1991.

[13] Lee M: Sliding mode controller with neural network and fuzzy logic, Proceedings of the IEEE International Conference on Neural Networks, USA, **4**, 2414–2417, (1997).

[14] R. A. Teixeira, A. D. Braga, and B. R. DeMenezes: Control of a Robotic Manipulator Using Artificial Neural Networks with On-line Adaptation, Neural Processing Letters, **12**, 19–31, (2000).

[15] F. L. Lewis, S. Jagannathan, and A. Yesildirek: Neural Network Control of Robot Manipulators and Nonlinear Systems, Tayor & Francis, 1999.

[16] S. Jagannathan, G. Galan: Adaptive critic neural network-based object grasping control using a three-finger gripper, IEEE Trans. Neural Networks **15**(2), 395–407 (2004).

[17] F. L. Lewis, A. Yesildirek, K. Liu: Multilayer neural-net robot controller with guaranteed tracking performance, IEEE Transactions on Neural Networks, **7**, 388–399, (1996).

[18] M. K. Ciliz: Adaptive control of robot manipulators with neural network based compensation of frictional uncertainties, Robotica, **23**, 159–167, (2005).

[19] H. D. Patino, R. Carelli, B.R. Kuchen: Neural networks for advanced control of robot manipulators, IEEE Transactions on Neural Networks, **13**(2), 343–354, (2002).

[20] Y. G. Tang, F.C. Sun, Z.Q. Sun: Neural network control of flexible-link manipulators using sliding mode, Neurocomputing, **70**(1–3), 288–295, (2006).

[21] B. Xian, D.M. Dawson, M.S. de Queiroz, J. Chen: A continuous asymptotic tracking control strategy for uncertain multi-input nonlinear systems, IEEE Transactions on Automatic Control, **49**(7), 1206–1211, (2004).

[22] C. Makkar, G. Hu, W. G. Sawyer, and W. E. Dixon: Lyapunov-based tracking control in the presence of uncertain nonlinear parameterizable friction, IEEE Trans. Automat. Control, **52**(10), (2007).

[23] Z. Cai, M. S. de Queiroz, and D. M. Dawson: Robust adaptive asymptotic tracking of nonlinear systems with additive disturbance, IEEE Trans. Automat. Control, **51**(3), (2006).

[24] P. M. Patre, W. MacKunis, W.E. Dixon, Asymptotic tracking for uncertain dynamic systems via a multilayer NN feedforward and RISE feedback control structure. IEEE Transactions on Automatic Control, **53**(9), 2180–2185, (2008).

[25] W. MacKunis, P. M. Patre, M. K. Kaiser, and W. E. Dixon: Asymptotic tracking for aircraft via robust and adaptive dynamic inversion methods. IEEE Trans. Cont. Syst. Technol., **18**(6), (2010).

[26] P. M. Patre, W. MacKunis, C. Makkar, and W. E. Dixon: Asymptotic tracking for systems with structured and unstructured uncertainties, IEEE Trans. Cont. Syst. Technol., **16**(2), (2008).

[27] S. Wang, H. Min, F. Sun, J. Zhang: Neural Network Control of Spacecraft Formation Using RISE Feedback, Advances in Neural Network Research and Applications, **67**, 521–528, (2010).

[28] W. E. Dixon, A. Behal, D. M. Dawson, and S. P. Nagarkatti, Nonlinear Control of Engineering Systems: a Lyapunov-Based Approach. Bostot, Birkhuser, (2003).

[29] E. Kim: Output feedback tracking control of robot manipulators with model uncertainty via adaptive fuzzy logic, IEEE Trans. Fuzzy Systems, **12**(3), 368–378, (2004).

[30] F. Lewis, J. Campos, and R. Selmic: Neuro-Fuzzy Control of Industrial Systems With Actuator Nonlinearities. Philadelphia, PA: SIAM, 2002.

[31] H. K. Khalil: Nonlinear System, third ed., Prentice-Hall, Upper Saddle River, NJ, 2002.